

The Tayler Instability in the Anelastic Approximation

J. GOLDSTEIN,^{1,2} R. H. D. TOWNSEND,^{1,2} AND E. G. ZWEIBEL^{1,3}

¹*Department of Astronomy, University of Wisconsin-Madison, 2535 Sterling Hall, 475 N. Charter Street, Madison, WI 53706, USA*

²*Kavli Institute for Theoretical Physics, University of California, Santa Barbara, CA 93106, USA*

³*Department of Physics, University of Wisconsin-Madison, 2535 Chamberlin Hall, 1150 University Avenue, Madison, WI 53706, USA*

Submitted to ApJ

ABSTRACT

The Tayler instability (TI) is a non-axisymmetric linear instability of an axisymmetric toroidal magnetic field in magneto-hydrostatic equilibrium (MHSE). Spruit (1999, 2002) has proposed that in a differentially rotating radiative region of a star, the TI drives a dynamo which generates magnetic fields that can efficiently transport angular momentum; a parameterized version of this dynamo has been implemented in stellar structure and evolution codes and shown to be important for determining interior spin. Numerical simulations, however, have yet to definitively demonstrate the operation of the dynamo. A criterion for the MHSE to develop the TI was derived using fully-compressible magnetohydrodynamics, while numerical simulations of dynamical processes in stars frequently use an anelastic approximation. This motivates us to derive a new anelastic Tayler instability (anTI) criterion. We find that some MHSE configurations unstable in the fully-compressible case, become stable in the anelastic case. We find and characterize the unstable modes of a simple family of cylindrical MHSE configurations using numerical calculations, and discuss the implications for fully non-linear anelastic simulations.

Keywords: dynamo — instabilities — magnetic fields — magnetohydrodynamics (MHD) — stars: magnetic field — stars: interiors

1. INTRODUCTION

The Tayler instability (TI; Tayler 1973; Markey & Tayler 1973, 1974; Acheson 1978; Pitts & Tayler 1985) is a non-axisymmetric linear instability of an axisymmetric toroidal magnetic field in magneto-hydrostatic equilibrium (MHSE). Spruit (1999) has argued that this instability is particularly important because it can manifest when other instabilities are suppressed by thermal stratification. Growth rates are on the order of the global Alfvén-wave crossing time, which is generally short compared to other stellar time scales, even for weak magnetic fields. These two qualities make the TI the most relevant magnetic instability of a toroidal magnetic field in MHSE, at least in a non-rotating star.

Spruit (1999, 2002) proposed that in a radiative region of a star, the TI generates a radial field displacement

which is then rewound by differential rotation back into a toroidal field, creating a dynamo loop. This Tayler-Spruit dynamo may generate a magnetic torque that is a significant mechanism of angular momentum transport inside stars. However, the existence and nature of the dynamo is currently debated through both analytical and numerical calculations. Analytically, various heuristic prescriptions have been developed to predict the magnitude of the magnetic torque (Spruit 1999, 2002; Heger et al. 2005; Denissenkov & Pinsonneault 2007). Most recently, Cantiello et al. (2014) showed that a heuristic prescription for the Tayler-Spruit dynamo implemented in the stellar evolution code Modules for Experiments in Stellar Astrophysics (MESA; Paxton et al. 2011, 2013, 2015, 2018) cannot fully explain the slow core rotation rates of RGB stars as observed by *Kepler*, but the models with the dynamo are in better agreement with observations than the models without. Numerically, non-linear magnetohydrodynamic (MHD) simulations have been ambiguous as to the manifesta-

tion of the dynamo at all (Braithwaite 2006; Zahn et al. 2007).

In view of the potential importance of the Tayler-Spruit dynamo for stars with radiative envelopes, the disagreement between the analytical predictions and the numerical results is troubling. An open question is whether the non-linear MHD simulations investigating the Tayler-Spruit dynamo used equilibrium models subject to the TI. Tayler (1973) developed a criterion for the TI using fully-compressible ideal MHD, while the simulations previously mentioned have used anelastic MHD. The anelastic approximation filters out sound waves, which are very short-period relative to stellar timescales and are therefore prohibitively expensive to compute.

The goal of this paper is to re-examine the TI in the anelastic approximation. We derive a new anelastic Tayler instability (anTI) criterion and apply it to a family of simple MHSE models to determine which are subject to the instability. We verify our results numerically using a modified version of the GYRE stellar oscillation code (Townsend & Teitler 2013), which solves a system of linearized anelastic MHD equations to calculate growth rates and eigenfunctions of unstable modes. We conclude that the anelastic case is more restrictive, but that the TI should be present in anelastic MHD simulations if the models used are unstable under the anTI criterion.

The rest of the paper is structured as follows. In §2 we give an overview of the energy principle — the method used to develop the instability criteria. In §3 we introduce the fully-compressible MHD equations and the Lantz-Braginsky-Roberts (LBR) anelastic approximation for MHD, a form that is valid in the isothermal atmosphere we assume in our later analysis. In §4 we develop a simple family of cylindrical MHSE models. In §5 we summarize the TI criterion derived from the energy principle, show our derivation of the new anTI criterion, and apply the criteria to our family of models. In §6 we compare the TI and anTI criteria to GYRE’s numerically calculated growth rates and eigenfunctions for unstable modes in our models, showing that the anTI criterion is correct in anelastic MHD. In §7 we conclude with considerations for future analytical and numerical work.

2. ENERGY PRINCIPLE

The instability analysis in Tayler (1973) was developed using the MHD energy principle of Bernstein et al. (1958), which gives the necessary and sufficient condition for an energy-conserving, ideal system in MHSE to be unstable to small displacements. Although the energy principle is widely used in studies of laboratory

and natural plasmas, we will need to modify it to accommodate the anelastic equations, so we briefly review it here.

The energy principle is based on being able to write the linearized equation of motion for the fluid displacement perturbation, ξ , in the form

$$\rho \frac{\partial^2 \xi}{\partial t^2} = \mathbf{F}(\xi), \quad (1)$$

where ξ is related to velocity perturbations \mathbf{u}' by

$$\mathbf{u}' = \frac{\partial \xi}{\partial t}, \quad (2)$$

and \mathbf{F} is a linear, self adjoint operator¹. Since equation (1) doesn’t explicitly depend on time, we look for separable solutions of the form

$$\xi(t) \propto \exp i\omega t, \quad (3)$$

where ω is an angular frequency. It follows from the self adjointness property that ω^2 is real; $\omega^2 < 0$ signifies instability, with an exponential growth rate $\lambda = |\omega|$.

It can be shown that equation (1), together with the self adjointness property, leads to a conservation law which we identify with conservation of perturbation energy:

$$\frac{\partial}{\partial t} \left[\frac{1}{2} \int \rho \frac{\partial \xi}{\partial t} \cdot \frac{\partial \xi}{\partial t} d\tau - \frac{1}{2} \int \xi \cdot \mathbf{F}(\xi) d\tau \right] = 0. \quad (4)$$

The first term in brackets in equation (4) is the kinetic energy δK , while the second represents the potential energy

$$\delta W = -\frac{1}{2} \int \xi \cdot \mathbf{F}(\xi) d\tau. \quad (5)$$

Equation (4) shows that $\delta K + \delta W$ is constant in time. Since for an unstable mode, both δK and δW grow exponentially in magnitude with time, and δK is positive definite, δW must be negative. This is the basis of the energy principle.

The energy principle has both advantages and disadvantages compared to solving for the eigenvalues ω^2 of equation (1). The advantage is that it is often easier to minimize δW , or even evaluate it for a set of trial functions, than to solve the coupled set of differential equations corresponding to the eigenvalue problem and hope to capture all modes. The disadvantage is that the energy principle yields at best the lowest mode (obtained by rigorous minimization of δW) rather than the whole spectrum of stable and unstable modes.

¹ By self adjointness we mean $\int \xi \cdot \mathbf{F}(\eta) d\tau = \int \eta \cdot \mathbf{F}(\xi) d\tau$ for displacement vectors ξ, η that obey suitable boundary conditions.

3. FULLY COMPRESSIBLE AND ANELASTIC IDEAL MHD

Fully compressible, isentropic, ideal MHD is described by the conservation equations for mass, momentum, and entropy, together with Faraday-Maxwell's Law (combined with Ohm's Law), Ampère's Law, and Gauss' Law for magnetism,

$$\frac{\partial \rho}{\partial t} + \nabla \cdot (\rho \mathbf{u}) = 0, \quad (6)$$

$$\frac{\partial \mathbf{u}}{\partial t} + \mathbf{u} \cdot \nabla \mathbf{u} = -\frac{1}{\rho} \nabla P + \mathbf{g} + \frac{\mathbf{J} \times \mathbf{B}}{\rho c}, \quad (7)$$

$$\frac{\partial S}{\partial t} + \mathbf{u} \cdot \nabla S = 0, \quad (8)$$

$$\frac{\partial \mathbf{B}}{\partial t} = \nabla \times (\mathbf{u} \times \mathbf{B}), \quad (9)$$

$$\mathbf{J} = \frac{c}{4\pi} \nabla \times \mathbf{B}, \quad (10)$$

$$\nabla \cdot \mathbf{B} = 0. \quad (11)$$

Here, \mathbf{u} , ρ , P , S , \mathbf{g} , \mathbf{B} and \mathbf{J} are the fluid velocity, density, pressure, specific entropy, gravitational acceleration, magnetic field and current density, respectively. The pressure, density and specific entropy are assumed to be related by the equation of state

$$\rho = \rho(S, P), \quad (12)$$

which for simplicity we assume to follow ideal-gas behavior.

In order to model the evolution of small perturbations of a static equilibrium state, we decompose the dependent variables into the sum of a background value (denoted by the subscript 0), and a perturbed value (denoted by a prime):

$$\begin{aligned} \mathbf{u} &= \mathbf{u}', \\ P &= P_0 + P', \\ \rho &= \rho_0 + \rho', \\ S &= S_0 + S', \\ \mathbf{B} &= \mathbf{B}_0 + \mathbf{B}', \\ \mathbf{J} &= \mathbf{J}_0 + \mathbf{J}'. \end{aligned} \quad (13)$$

The background values obey the MHSE condition

$$\frac{\nabla P_0}{\rho_0} = \mathbf{g} + \frac{\mathbf{J}_0 \times \mathbf{B}_0}{\rho_0 c}, \quad (14)$$

the equilibrium current equation

$$\mathbf{J}_0 = \frac{c}{4\pi} \nabla \times \mathbf{B}_0, \quad (15)$$

and a gradient relation that follows from the equation of state (12),

$$\frac{\nabla \rho_0}{\rho_0} = \frac{\nabla P_0}{\gamma P_0} - \frac{\nabla S_0}{c_P}, \quad (16)$$

where c_P is the specific heat at constant pressure and γ is the usual ratio of specific heats. Likewise, the perturbed values satisfy the linearized ideal MHD equations that follow when we substitute the expressions (13) into equations (6–11), subtract the background state, and discard terms that are second- or higher-order in perturbed quantities:

$$\frac{\partial \rho'}{\partial t} + \nabla \cdot (\rho_0 \mathbf{u}') = 0, \quad (17)$$

$$\frac{\partial \mathbf{u}'}{\partial t} = -\frac{\nabla P'}{\rho_0} + \frac{\rho'}{\rho_0} \mathbf{g} + \left(\frac{\mathbf{J}' \times \mathbf{B}_0 + \mathbf{J}_0 \times \mathbf{B}'}{\rho_0 c} \right), \quad (18)$$

$$\frac{\partial S'}{\partial t} + \mathbf{u}' \cdot \nabla S_0 = 0, \quad (19)$$

$$\frac{\partial \mathbf{B}'}{\partial t} = \nabla \times (\mathbf{u}' \times \mathbf{B}_0), \quad (20)$$

$$\mathbf{J}' = \frac{c}{4\pi} (\nabla \times \mathbf{B}'), \quad (21)$$

$$\nabla \cdot \mathbf{B}' = 0. \quad (22)$$

Numerical MHD simulations that are relevant on stellar scales of interest frequently use an anelastic approximation,

$$\nabla \cdot (\rho_0 \mathbf{u}') = 0, \quad (23)$$

which filters out fast, high-frequency sound waves unimportant on stellar scales, while keeping slower internal gravity waves. The anelastic approximation is technically valid only for adiabatically stratified systems ($\nabla S_0 = 0$), but is now used to study problems such as penetrative convection and interface dynamos that include stably stratified regions. In such contexts, Brown et al. (2012) studied energy conservation in three widely used forms of the anelastic equations. They showed that one, the so-called Lantz-Braginskii-Roberts (LBR) formulation (Lantz 1992; Braginsky & Roberts 1995) conserves energy, while the others conserve a related but distinct pseudo-energy. Therefore, we consider the LBR formulation to be the best candidate for analyzing the Taylor instability in the anelastic approximation, and study only that version in this paper. However, as we will see, the energy principle has to be modified even for the LBR formulation.

The LBR formulation re-writes the linear momentum equation in terms of entropy and a reduced pressure perturbation,

$$\varpi' \equiv \frac{P'}{\rho_0}, \quad (24)$$

neglecting a term $\varpi' \nabla (S_0/c_P)$. Although Brown et al. (2012) neglected the effect of magnetic fields, it can be shown by recapitulating their analysis that neglecting *all* terms proportional to ϖ' (but not its gradient) in the

linearized momentum equation preserves energy conservation in an isothermal atmosphere, even in the presence of magnetic fields.

We develop an LBR version of the linearized momentum equation (18) by eliminating the density perturbation using the linearized equation of state,

$$\frac{\rho'}{\rho_0} = \frac{1}{\gamma} \frac{P'}{P_0} - \frac{S'}{c_P}, \quad (25)$$

and likewise eliminating the background pressure gradient ∇P_0 using the MHSE condition (14). The linearized momentum equation then becomes

$$\frac{\partial \mathbf{u}'}{\partial t} = -\nabla \varpi' - \frac{S'}{c_P} \mathbf{g} + \left(\frac{\mathbf{J}' \times \mathbf{B}_0 + \mathbf{J}_0 \times \mathbf{B}'}{\rho_0 c} \right), \quad (26)$$

where, as discussed above, we have dropped all terms proportional to ϖ' . The linearized LBR anelastic MHD equations are then composed of equations (19–23) and (26).

4. EQUILIBRIUM MODEL

Taylor (1973) assumed a 2D, axisymmetric toroidal magnetic field in a non-rotating stratified plasma in which all equilibrium quantities are functions only of the cylindrical radial (r) and axial (z) coordinates. Here we examine a reduced case in 1D, in which the equilibrium depends only on r . We assume an isothermal atmosphere and a constant ratio of gas pressure to magnetic pressure. The equilibrium is then described by

$$\mathbf{B}_0(r) = B_\phi(r) \hat{\phi}, \quad (27)$$

$$P_0(r) = a^2 \rho_0(r), \quad (28)$$

$$\mathbf{g}(r) = g_r(r) \hat{r}, \quad (29)$$

$$\beta = \frac{8\pi P_0}{B_\phi^2}, \quad (30)$$

where \hat{r} and $\hat{\phi}$ are the unit vectors in the r and ϕ directions, respectively; B_ϕ is the toroidal magnetic field; g_r is the radial gravity; β is the constant ratio of gas to magnetic pressure; and a is the constant isothermal sound speed. This model can be extended to include rotation with a constant ratio of centrifugal to gravitational acceleration, but we only consider the non-rotating case here, as it is the only case to which the MHD energy principle applies.

As a specific realization of our equilibrium, we consider a configuration where the gravity is provided by a line mass on the axis of symmetry,

$$g_r(r) = -\frac{qa^2}{r}, \quad (31)$$

where $q \geq 0$ is a dimensionless gravitational strength parameter. Then the MHSE condition (14) reduces to

$$\frac{d}{dr} \left(P_0 + \frac{B_\phi^2}{8\pi} \right) + \frac{B_\phi^2}{4\pi r} + \frac{qP_0}{r} = 0. \quad (32)$$

We can solve for the background pressure profile by rewriting this equation as

$$\frac{dP_0}{P_0} = -\alpha \frac{dr}{r}, \quad (33)$$

where

$$\alpha = \frac{2 + q\beta}{1 + \beta}. \quad (34)$$

Integrating equation (33), the background pressure for $r > 0$ is found as

$$P_0 = P_{0,0} \left(\frac{r}{r_0} \right)^{-\alpha}, \quad (35)$$

where $P_{0,0}$ and r_0 are a fiducial pressure and radius, respectively. These two parameters, together with a , β , γ and q , completely specify our model.

It can be shown that for $\alpha < 2$, the magnetic tension term dominates the magnetic pressure term, meaning that the equilibrium is both magnetically and gravitationally confined. To satisfy $\alpha < 2$, from equation (34), the gravitational parameter must be $q < 1$. For stars, of course, we expect that the magnetic field is relatively weak and that the equilibrium is close to hydrostatic, whether the magnetic field provides pressure support through its negative gradient or confinement through tension.

5. INSTABILITY ANALYSIS

5.1. Fully-Compressible Analysis

Taylor (1973) derived the TI criterion using a fully-compressible MHD form of the energy principle (see §2). Here, we briefly recapitulate his analysis. First, we integrate equations (17) and (20) with respect to time to obtain explicit expressions for the density, magnetic field and current perturbations in terms of the displacement vector ξ ,

$$\rho' = -\nabla \cdot (\rho_0 \xi), \quad (36)$$

$$\mathbf{B}' = \nabla \times (\xi \times \mathbf{B}_0), \quad (37)$$

$$\mathbf{J}' = \frac{c}{4\pi} \nabla \times [\nabla \times (\xi \times \mathbf{B}_0)]. \quad (38)$$

The linearized equation of state (25) leads to a corresponding expression for the pressure perturbation,

$$P' = -\gamma P_0 \nabla \cdot \xi - \xi \cdot \nabla P_0. \quad (39)$$

By substituting these expressions into the linearized momentum equation (18), the force operator introduced in equation (1) is found to be

$$\mathbf{F}(\boldsymbol{\xi}) = \nabla(\gamma P_0 \nabla \cdot \boldsymbol{\xi} - \boldsymbol{\xi} \cdot \nabla P_0) - \nabla \cdot (\rho_0 \boldsymbol{\xi}) \mathbf{g} + \frac{1}{4\pi} [(\nabla \times \mathbf{B}') \times \mathbf{B}_0 + (\nabla \times \mathbf{B}_0) \times \mathbf{B}']. \quad (40)$$

Kulsrud (1964) demonstrated that this force operator is self-adjoint under boundary conditions

$$\boldsymbol{\xi} \cdot \hat{\mathbf{n}} = 0, \quad \mathbf{B}_0 \cdot \hat{\mathbf{n}} = 0, \quad (41)$$

that correspond to rigid, perfectly-conducting walls; here, $\hat{\mathbf{n}}$ is the unit surface normal vector of the boundary.

Taking the scalar product of equation (40) with $\boldsymbol{\xi}$, and integrating over volume, leads via equation (5) to the potential energy

$$\delta W = \frac{1}{2} \int \left[\frac{\mathbf{B}'^2}{4\pi} - \frac{\mathbf{J}_0 \cdot (\mathbf{B}' \times \boldsymbol{\xi})}{c} + \gamma P_0 (\nabla \cdot \boldsymbol{\xi})^2 + (\boldsymbol{\xi} \cdot \nabla P_0) \nabla \cdot \boldsymbol{\xi} + (\boldsymbol{\xi} \cdot \mathbf{g}) \nabla \cdot (\rho_0 \boldsymbol{\xi}) \right] d\tau \quad (42)$$

where we have made use of the boundary conditions (41) to eliminate surface integrals involving $\boldsymbol{\xi} \cdot \hat{\mathbf{n}}$ and $\mathbf{B}_0 \cdot \hat{\mathbf{n}}$.

Following Tayler (1973), we write the fluid displacement vector in cylindrical coordinates as

$$\begin{bmatrix} \xi_r \\ \xi_\phi \\ \xi_z \end{bmatrix} = \begin{bmatrix} X \cos m\phi \\ -(Y/m) \sin m\phi \\ Z \cos m\phi \end{bmatrix}, \quad (43)$$

where X, Y, Z are real functions of r and z , and the integer m is an azimuthal wavenumber. With these definitions, and assuming the MHSE configuration we introduce via equations (27–30), we evaluate the ϕ part of the integral in equation (42) to obtain

$$\delta W = \frac{1}{8} \int \left\{ \frac{m^2 B_\phi^2}{r^2} (X^2 + Z^2) + C_{XZ}^2 - \frac{1}{r} \frac{\partial}{\partial r} (r B_\phi) X C_{XZ} - \frac{B_\phi}{r^2} \frac{\partial}{\partial r} (r B_\phi) X Y + 4\pi \gamma P_0 C_{XYZ}^2 + 4\pi g_r X^2 \frac{d\rho_0}{dr} + 4\pi X \left(\frac{dP_0}{dr} + \rho g_r \right) C_{XYZ} \right\} r dr dz. \quad (44)$$

where we introduce

$$C_{XZ} \equiv \frac{\partial}{\partial r} (B_\phi X) + B_\phi \frac{\partial Z}{\partial z}, \quad (45)$$

$$C_{XYZ} \equiv \frac{1}{r} \frac{\partial}{\partial r} (r X) - \frac{Y}{r} + \frac{\partial Z}{\partial z} \quad (46)$$

to simplify the expression. As discussed by Tayler (1973), δW is least positive when $m = 1$. Adopting this value, we further minimize δW with respect to Y by solving

$$\frac{\partial \delta W}{\partial Y} = 0 \quad (47)$$

to obtain

$$\frac{Y}{r} = \frac{1}{r} \frac{\partial}{\partial r} (r X) + \frac{\partial Z}{\partial z} + \frac{\rho_0 g_r}{\gamma P_0} X. \quad (48)$$

Substituting this back into equation (44), and setting $m = 1$, we obtain the minimized potential energy as

$$\delta W_{\min} = \frac{1}{8} \int \left\{ B_\phi^2 \left[r \frac{d}{dr} \left(\frac{X}{r} \right) + \frac{dZ}{dz} \right]^2 + \left[4\pi g_r \left(\frac{d\rho_0}{dr} - \frac{g_r \rho_0^2}{\gamma P_0} \right) - \frac{B_\phi^2}{r^2} - \frac{1}{r} \frac{d}{dr} B_\phi^2 \right] X^2 + \frac{B_\phi^2}{r^2} Z^2 \right\} r dr dz. \quad (49)$$

A necessary condition for δW to be negative, for any X and Z , is that the bracketed term proportional to X^2 be negative; that is,

$$g_r \left(\frac{d\rho_0}{dr} - \frac{g_r \rho_0^2}{\gamma P_0} \right) - \frac{B_\phi^2}{4\pi r^2} - \frac{1}{r} \frac{d}{dr} \frac{B_\phi^2}{4\pi} < 0, \quad (50)$$

This is the Tayler instability (TI) criterion for fully-compressible MHD; allowing for factors of 4π that arise from our choice of electromagnetic units, it is in agreement with equation 2.20 of Tayler (1973) when g_z is set to zero. As Tayler demonstrated, this criterion is both necessary and sufficient for instability to develop.

For the specific realization of the equilibrium that follows from equations (31–35), the instability criterion (50) reduces to

$$q \left(\alpha - \frac{q}{\gamma} \right) + \frac{2}{\beta} (\alpha - 1) < 0. \quad (51)$$

5.2. Constrained Analysis

We now consider how to implement the anelastic constraint in our analysis. This constraint removes the freedom to choose a Y that minimizes δW ; instead, we must set

$$\frac{Y}{r} = \frac{1}{r} \frac{\partial(rX)}{\partial r} + \frac{\partial Z}{\partial z} + \frac{1}{\rho_0} \frac{d\rho_0}{dr} X \quad (52)$$

to ensure that equation (23) is satisfied. We repeat the analysis of the preceding section, but using this expression in place of equation (48), to obtain the instability

criterion

$$g_r \left(\frac{d\rho_0}{dr} - \frac{g_r \rho_0^2}{\gamma P_0} \right) - \frac{B_\phi^2}{4\pi r^2} - \frac{1}{r} \frac{d}{dr} \frac{B_\phi^2}{4\pi} + \frac{\gamma P_0}{\rho_0^2} \left(\frac{d\rho_0}{dr} - \frac{\rho_0^2 g_r}{\gamma P_0} \right)^2 < 0 \quad (53)$$

We refer to this as the ‘constrained TI’ (cTI) criterion; it resembles the fully-compressible criterion (50) but with an additional term. Since this term is positive-definite, the constrained TI criterion always predicts less instability than the original criterion. This qualitatively makes sense, because anelasticity imposes a constraint on the potential energy that full compressibility does not.

For the equilibrium given by equations (31–35), the cTI criterion (53) reduces to

$$q \left(\alpha - \frac{q}{\gamma} \right) + \frac{2}{\beta} (\gamma - 1) + \gamma \left(\alpha - \frac{q}{\gamma} \right)^2 < 0; \quad (54)$$

As we demonstrate in Section 6, this constrained criterion under-predicts the extent of the TI found by numerical calculations employing the anelastic condition.

5.3. LBR Anelastic Analysis

The shortcomings of the cTI criterion motivate a more careful analysis, based on re-deriving the force operator from the LBR anelastic linearized momentum equation (26). First, we integrate equation (19) with respect to time to obtain

$$S' = -\xi \cdot \nabla S_0. \quad (55)$$

Substituting this expression and equations (36–39) into the linearized momentum equation (26), the LBR anelastic force operator is derived as

$$\mathbf{F}_{\text{LBR}}(\xi) = -\rho_0 \nabla \varpi' - \rho_0 \mathbf{g} \cdot \left[\frac{\nabla P_0}{\gamma P_0} - \frac{\nabla \rho_0}{\rho_0} \right] + \frac{1}{4\pi} [(\nabla \times \mathbf{B}') \times \mathbf{B}_0 + (\nabla \times \mathbf{B}_0) \times \mathbf{B}'], \quad (56)$$

where we have used equation (16) to eliminate the background entropy gradient ∇S_0 . This operator is self-adjoint under the same boundary conditions (41) as applied before.

We next repeat the analysis of Section 5.1, but using equations (52,56) in place of (40,48), to obtain the condition for instability:

$$g_r \left(\frac{d\rho_0}{dr} - \frac{g_r \rho_0^2}{\gamma P_0} \right) - \frac{B_\phi^2}{4\pi r^2} - \frac{1}{r} \frac{d}{dr} \frac{B_\phi^2}{4\pi} - \left(\frac{B_\phi^2}{4\pi r} + \frac{1}{4\pi} \frac{dB_\phi}{dr} \right) \frac{B_\phi}{\rho_0} \frac{d\rho_0}{dr} < 0 \quad (57)$$

(this is the necessary condition; we assume without proof that it is also sufficient). This anelastic TI (anTI) criterion is the principal result of this paper. For the equilibrium given by equations (31–35), the anTI criterion reduces to

$$q \left(\alpha - \frac{\alpha}{\gamma} \right) + \frac{2}{\beta} \left(\frac{\alpha^2}{2} - 2\alpha + 1 \right) < 0 \quad (58)$$

In the following section, we test this criterion via numerical calculations, to find that it correctly predicts the boundary of the TI in LBR anelastic MHD.

6. NUMERICAL INSTABILITY CALCULATIONS

In this section, we compare the analytic work in the preceding sections against numerical solutions of the linearized LBR anelastic MHD equations and boundary conditions. Details of our numerical technique are given in the Appendix; in brief, we modify the GYRE stellar oscillation code (Townsend & Teitler 2013) to find the modal eigenvalues and eigenfunctions.

We first focus on a MHSE configuration having $\beta = 5$, $q = 0.01$ and $\gamma = 5/3$; this choice of parameters ensures that we are looking at a robust instability, as we shall later show in a parameter study. We solve the linearized equations and boundary conditions on a spatial grid of 1,000 points, uniformly spanning the domain $[\tilde{r}_a, \tilde{r}_b] = [1, 1.5]$ (here, \tilde{r} is the dimensionless radius introduced in the Appendix). Assuming an azimuthal wavenumber $m = 1$ and an axial wavenumber $k = 25$, we search for modes having eigenvalues $\tilde{\omega}^2$ below $\tilde{\omega}_A^2$ evaluated at $\tilde{r} = \tilde{r}_b$ (see equation A17). These modes comprise an infinite family, in which each mode can uniquely be classified by a radial order n that counts the number of nodes n (excluding the endpoints) in the dimensionless radial displacement eigenfunction $\tilde{\xi}_r$. With this classification, an ordering by n is in one-to-one correspondence with an ordering by $\tilde{\omega}^2$, with the eigenvalue $\tilde{\omega}_0^2$ of the $n = 0$ (fundamental) mode being the least positive.

Figure 1 plots the dimensionless displacement eigenfunctions, $\tilde{\xi}_r$, $\tilde{\xi}_\phi$, and $\tilde{\xi}_z$, as a function of \tilde{r} for the three lowest-order modes ($n = 0, 1, 2$). Each plot is labeled at top-left by the corresponding eigenvalue $\tilde{\omega}_n^2$. From these eigenvalues, we see that the fundamental mode and first overtone ($n = 1$) are both unstable, with $\tilde{\omega}^2 < 0$. From the eigenfunctions, we see that the displacement in the azimuthal direction is greater than that in the radial direction, $|\tilde{\xi}_\phi| > |\tilde{\xi}_r|$, as predicted by Spruit (2002). This makes sense because displacement along the magnetic field lines on equipotential gravitational surfaces does not need to do work against the stratification.

We now explore how the mode eigenvalues depend on the axial wavenumber k . Keeping other parameters fixed

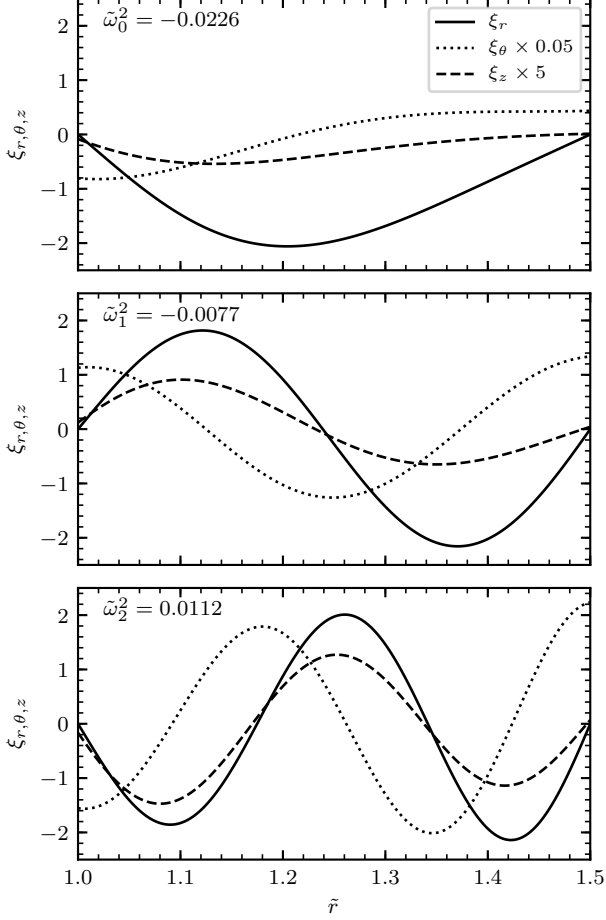


Figure 1. Dimensionless displacement eigenfunctions of the $n = 0, 1, 2$ modes (top to bottom), for an azimuthal wavenumber $m = 1$ and an axial wavenumber $k = 25$, and an equilibrium model having $\beta = 5$, $q = 0.01$ and $\gamma = 5/3$. In each panel, the eigenfunctions are normalized such that the root-mean-square value of ξ_r is unity. The plots are labeled with the corresponding eigenvalue $\tilde{\omega}_n^2$; negative values for the $n = 0$ and $n = 1$ modes indicates that they are unstable.

at the values given above, Fig. 2 plots the eigenvalues of unstable modes as a function of k . The plot shows that in order for a mode to become unstable, k must exceed some finite threshold k_n . Above this threshold, the eigenvalue decreases monotonically with k , approaching an asymptotic limit as $k \rightarrow \infty$. This is similar behavior to that found by Pitts & Tayler (1985) for a uniform-density incompressible fluid without gravity. In a non-ideal fluid with one or more forms of diffusion (thermal, viscous, or resistive) diffusive damping is expected to reduce the instability of modes at high k , leading to a minimal $\tilde{\omega}^2 < 0$ (i.e., maximal growth rate) at large but finite k .

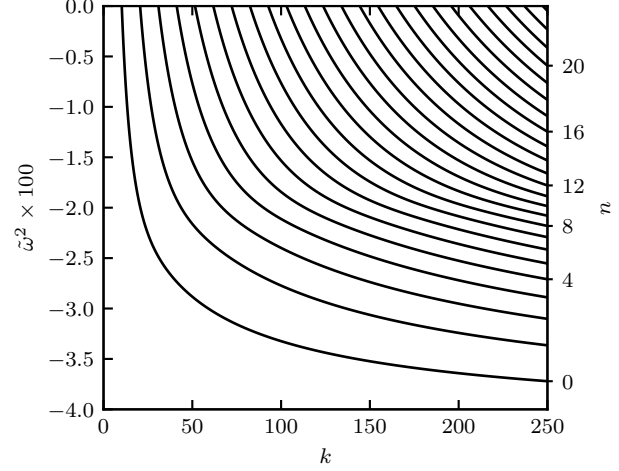


Figure 2. Eigenvalues $\tilde{\omega}^2$ plotted as a function of axial wavenumber k , for an azimuthal wavenumber $m = 1$ and an equilibrium model having $\beta = 5$, $q = 0.01$ and $\gamma = 5/3$. Selected modes are labeled at right with their radial order n .

Because the fundamental mode is the most unstable at any k , we can use it as a proxy for the onset of the TI. Accordingly, we can evaluate the minimal eigenvalue $\tilde{\omega}_{\min}^2$, over all modes, as the limiting value of the fundamental-mode eigenvalue in the limit $k \rightarrow \infty$:

$$\tilde{\omega}_{\min}^2 = \lim_{k \rightarrow \infty} \tilde{\omega}_0^2. \quad (59)$$

When $\tilde{\omega}_{\min}^2 < 0$, the maximal exponential growth rate of the Tayler instability is then given by

$$\lambda_{\max} = \frac{a|\tilde{\omega}_{\min}|}{r_0}. \quad (60)$$

Because our numerical calculations are restricted to finite values of k , we estimate the limit on the right-hand side of equation (59) by evaluating $\tilde{\omega}_0^2$ at $k = 1000$ and $k = 2000$, and then linearly extrapolating in inverse wavenumber k^{-1} to find the eigenvalue at $k^{-1} \rightarrow 0$.

We apply this approach to evaluate $\tilde{\omega}_{\min}^2$ for a grid of equilibrium models spanning $1 \leq \beta \leq 30$ and $0.00 \leq q \leq 0.40$. In all cases, we assume an azimuthal wavenumber $m = 1$ and $\gamma = 5/3$. Fig. 3 shows a contour map of the resulting values. Plotted over the map are the stability boundaries predicted by the fully-compressible TI criterion (equation 51), the cTI criterion (equation 54) and anTI criterion (equation 58). The fully compressible criterion over-predicts the extent of the instability seen in the numerical calculations, while the cTI criterion under-predicts it. Only the anTI criterion correctly predicts the stability boundary $\tilde{\omega}_{\min}^2 = 0$, confirming that it is the correct one to use for LBR anelastic MHD.

In his dynamo models, Spruit (1999, 2002) assumes that the growth rate of the TI is of the order $\lambda \approx \omega_A$

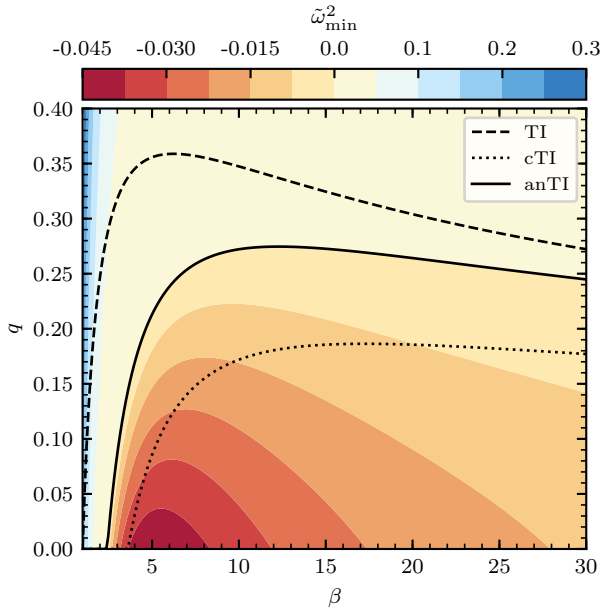


Figure 3. Contour map of the minimal eigenvalue $\tilde{\omega}_{\min}^2$, plotted across the β - q plane for an azimuthal wavenumber $m = 1$ and equilibrium models having $\gamma = 5/3$. Regions where $\tilde{\omega}_{\min}^2 < 0$ are unstable to the Tayler instability. The three black lines show the stability boundaries for the fully compressible TI criterion, the constrained criterion (cTI) and the anelastic criterion (anTI). Only the anTI criterion correctly predicts the $\tilde{\omega}_{\min}^2 = 0$ stability boundary.

in the limit where the rotation angular frequency Ω is small compared to the Alfvén frequency ω_A defined by

$$\omega_A^2 = \frac{2m^2 a^2}{\beta r^2}. \quad (61)$$

To compare this assumption against our calculations, we write the ratio of growth rate to Alfvén frequency as

$$\frac{\lambda}{\omega_A} = |\omega| \sqrt{\frac{\beta r^2}{2m^2 a^2}} \lesssim |\tilde{\omega}_{\min}| \sqrt{\frac{\beta(\tilde{r}_a + \tilde{r}_b)^2}{8m^2}}, \quad (62)$$

where the second (in)equality follows from setting $|\tilde{\omega}| = |\tilde{\omega}_{\min}|$, and evaluating the ratio at the midpoint $\tilde{r} = (\tilde{r}_a + \tilde{r}_b)/2$ of the calculation domain. For modes with azimuthal order $m = 1$, we find this ratio has an average value $\lambda/\omega_A \approx 0.27$ over the unstable region plotted in Fig. 3, and a maximal value $\lambda/\omega_A \approx 0.42$. These are both moderately smaller than the $\lambda/\omega_A \approx 1$ assumed by Spruit (1999, 2002). Therefore, future studies involving anelastic MHD simulations of the TI should recognize that the growth rate can be smaller than ω_A , and adjust expectations accordingly.

7. CONCLUSION

The TI is of great interest in the radiative regions of stars because, with differential rotation, it may contribute to forming and maintaining a magnetic field dynamo. The resulting torques could transport significant angular momentum (Spruit 2002; Heger et al. 2005; Cantiello et al. 2014). However, attempts to simulate the growth and saturation of the TI in stellar models have led to indeterminate results.

The TI criterion was derived using fully compressible MHD, but simulations of fluid dynamics in stellar interiors generally use some version of the anelastic or pseudo-incompressible approximations, which suppress acoustic waves with much shorter periods than stellar timescales. The goal of this paper was to address the gap between fully-compressible linear theory and anelastic non-linear simulations.

We did this by modifying the classic MHD energy principle (Bernstein et al. 1958) according to LBR anelastic MHD, which — based on the work of Brown et al. (2012) — we regard as the most promising of several anelastic schemes. We derived a version of the MHD energy principle that yields a stability criterion (eqn. 57) in excellent agreement with solutions of the eigenvalue problem calculated using the GYRE code. Our test bed was a family of cylindrically symmetrical magnetohydrostatic equilibria with toroidal magnetic field and gravity supplied by a line mass (§4). Our results show that the instability still exists in LBR anelastic MHD, but in a more restricted part of parameter space than the fully-compressible case. This is because the energy principle is based on minimizing the potential energy of the system, and anelasticity introduces a constraint which precludes full minimization. However, we conclude that the instability should manifest in anelastic LBR MHD simulations if the models used are unstable under the anTI criterion.

We found that the amplitude of the displacement in the horizontal direction is greater than the displacement in the radial direction, as predicted by Spruit (2002). We also found that the largest growth rates calculated by GYRE are somewhat smaller than predicted for slow rotators by Spruit (2002).

We are limited in addressing discrepancies between our calculations and heuristic predictions of the saturated state because our analysis and numerical calculations are in the linear regime and lack rotation or dissipative effects, both of which are key ingredients in the proposed instability-driven dynamo (Spruit 2002). We are unable to predict the non-linear growth rate and amplitude of the instabilities without taking those physical effects into consideration. That is beyond the scope of this work, but it is an open question for future work.

Our family of cylindrical models can be implemented in anelastic MHD simulations. Such simulations could verify the linear analysis and calculations that we performed, and determine how non-linear effects impact the growth rate and amplitude of the instability. Choosing models that are unstable under the anTI criterion, and including differential rotation, anelastic MHD simulations could more accurately test the the Tayler-Spruit dynamo and its significance as a mechanism for angular momentum transport in stellar evolution.

8. ACKNOWLEDGEMENTS

Our work made possible through the collaborative effort of the Supernova Progenitors, Internal Dynamics and Evolution Research (SPIDER) network, supported via NASA TCAN program grant NNX14AB55G. We also acknowledge support from NSF grants AST-1716436, PHY-1748958 and ACI-1663696, and from the Wisconsin Alumi Research Foundation. We thank Ryan Orvedahl and Benjamin Brown for their help using Dedalus (<http://dedalus-project.org>) to verify the initial GYRE calculations, and Erin Boettcher for her thorough review. EGZ thanks the University of Chicago for hospitality during the completion of this manuscript.

REFERENCES

Acheson, D. J. 1978, Philosophical Transactions of the Royal Society of London Series A, 289, 459

Bernstein, I. B., Frieman, E. A., Kruskal, M. D., & Kulsrud, R. M. 1958, Proceedings of the Royal Society of London A: Mathematical, Physical and Engineering Sciences, 244, 17. <http://rspa.royalsocietypublishing.org/content/244/1236/17>

Braginsky, S. I., & Roberts, P. H. 1995, Geophysical and Astrophysical Fluid Dynamics, 79, 1

Braithwaite, J. 2006, A&A, 449, 451

Brown, B. P., Vasil, G. M., & Zweibel, E. G. 2012, ApJ, 756, 109

Cantiello, M., Mankovich, C., Bildsten, L., Christensen-Dalsgaard, J., & Paxton, B. 2014, ApJ, 788, 93

Denissenkov, P. A., & Pinsonneault, M. 2007, ApJ, 655, 1157

Heger, A., Woosley, S. E., & Spruit, H. C. 2005, ApJ, 626, 350

Kulsrud, R. 1964, in Astrophysics Today, Vol. 63, Advanced Plasma Theory, ed. M. N. Rosenbluth, 54

Lantz, S. R. 1992, PhD thesis, CORNELL UNIVERSITY.

Markey, P., & Tayler, R. J. 1973, MNRAS, 163, 77

—. 1974, MNRAS, 168, 505

Paxton, B., Bildsten, L., Dotter, A., et al. 2011, ApJS, 192, 3

Paxton, B., Cantiello, M., Arras, P., et al. 2013, ApJS, 208, 4

Paxton, B., Marchant, P., Schwab, J., et al. 2015, ApJS, 220, 15

Paxton, B., Schwab, J., Bauer, E. B., et al. 2018, ApJS, 234, 34

Pitts, E., & Tayler, R. J. 1985, MNRAS, 216, 139

Spruit, H. C. 1999, A&A, 349, 189

—. 2002, A&A, 381, 923

Tayler, R. J. 1973, MNRAS, 161, 365

Townsend, R. H. D., & Teitler, S. A. 2013, MNRAS, 435, 3406

Zahn, J.-P., Brun, A. S., & Mathis, S. 2007, A&A, 474, 145

APPENDIX

A. NUMERICAL TECHNIQUE

To calculate numerical solutions of the LBR anelastic equations (19–23,26), we first undertake a separation of variables in space and time, by writing perturbed quantities in the form

$$\begin{pmatrix} \xi_r \\ \xi_\phi \\ \xi_z \end{pmatrix} = r_0 \operatorname{Re} \left\{ \begin{pmatrix} \tilde{\xi}_r \\ i\tilde{\xi}_\phi \\ i\tilde{\xi}_z \end{pmatrix} \exp[i(m\phi + kz/r_0 + \omega t)] \right\} \quad (\text{A1})$$

$$\begin{pmatrix} B'_r \\ B'_\phi \\ B'_z \end{pmatrix} = \sqrt{\frac{8\pi P_0}{\beta}} \operatorname{Re} \left\{ \begin{pmatrix} i\tilde{B}'_r \\ \tilde{B}'_\phi \\ \tilde{B}'_z \end{pmatrix} \exp[i(m\phi + kz/r_0 + \omega t)] \right\} \quad (\text{A2})$$

$$\begin{pmatrix} J'_r \\ J'_\phi \\ J'_z \end{pmatrix} = \frac{c}{4\pi r_0} \sqrt{\frac{8\pi P_0}{\beta}} \operatorname{Re} \left\{ \begin{pmatrix} i\tilde{J}'_r \\ \tilde{J}'_\phi \\ \tilde{J}'_z \end{pmatrix} \exp[i(m\phi + kz/r_0 + \omega t)] \right\}. \quad (\text{A3})$$

$$\Pi' = \frac{P_0}{\rho_0} \operatorname{Re} \left\{ \tilde{\Pi}' \exp[i(m\phi + kz/r_0 + \omega t)] \right\} \quad (\text{A4})$$

$$S' = c_P \operatorname{Re} \left\{ \tilde{S}' \exp[i(m\phi + kz/r_0 + \omega t)] \right\} \quad (\text{A5})$$

In these expressions, all quantities with a tilde ($\tilde{\cdot}$) are dimensionless real functions of r , to be determined numerically; the integer m is the azimuthal wavenumber introduced in Section (5.1), and the real number k is the axial wavenumber. Here, we choose to work with

$$\Pi' = \varpi' + \frac{B_\phi B'_\phi}{4\pi\rho_0}. \quad (\text{A6})$$

rather than the reduced pressure ϖ , as this allows \tilde{J}'_ϕ and \tilde{J}'_z to be decoupled from the other dependent variables, reducing the differential order of the system from four to two.

With these definitions, and assuming the equilibrium we introduce in Section 4, we write the linearized equations in the form

$$\frac{dv}{d\tilde{r}} = \mathbf{A}_{vv}v + \mathbf{A}_{vw}w \quad (\text{A7})$$

$$0 = \mathbf{A}_{wv}v + \mathbf{A}_{ww}w \quad (\text{A8})$$

where $\tilde{r} \equiv r/r_0$ is the independent variable, and the vectors

$$v = \begin{pmatrix} \tilde{\xi}_\phi \\ \tilde{\xi}_z \\ \tilde{B}'_r \\ \tilde{B}'_\phi \\ \tilde{B}'_z \\ \tilde{J}'_r \\ \tilde{S}' \end{pmatrix}, \quad w = \begin{pmatrix} \tilde{\xi}_r \\ \tilde{\Pi}' \end{pmatrix}, \quad (\text{A9})$$

contain the dependent variables. The Jacobian matrices in equations (A7) and (A8) are given by

$$\mathbf{A}_{vv} = \begin{pmatrix} \frac{\alpha-1}{\tilde{r}} & 0 \\ \tilde{\omega}^2 & 0 \end{pmatrix}, \quad (\text{A10})$$

$$\mathbf{A}_{vw} = \begin{pmatrix} \frac{m}{\tilde{r}} & k & 0 & 0 & 0 & 0 & 0 \\ 0 & 0 & -\frac{2m}{\beta\tilde{r}} & \frac{2(\alpha-2)}{\beta\tilde{r}} & 0 & 0 & \frac{q}{\tilde{r}} \end{pmatrix}, \quad (\text{A11})$$

$$\mathbf{A}_{wv} = \begin{pmatrix} 0 & -\frac{m}{\tilde{r}} \\ 0 & -k \\ \frac{m}{\tilde{r}} & 0 \\ \frac{2-\alpha}{2\tilde{r}} & 0 \\ 0 & 0 \\ 0 & 0 \\ \frac{\alpha(\gamma-1)}{\gamma\tilde{r}} & 0 \end{pmatrix}, \quad (\text{A12})$$

$$\mathbf{A}_{ww} = \begin{pmatrix} \tilde{\omega}^2 & 0 & \frac{2-\alpha}{\beta\tilde{r}} & \frac{2m}{\beta\tilde{r}} & 0 & 0 & 0 \\ 0 & \tilde{\omega}^2 & 0 & \frac{2k}{\beta} & 0 & \frac{2}{\beta} & 0 \\ 0 & 0 & -1 & 0 & 0 & 0 & 0 \\ -\frac{m}{\tilde{r}} & 0 & 0 & -1 & 0 & 0 & 0 \\ 0 & -\frac{m}{\tilde{r}} & 0 & 0 & -1 & 0 & 0 \\ 0 & 0 & 0 & -k & \frac{m}{\tilde{r}} & -1 & 0 \\ 0 & 0 & 0 & 0 & 0 & 0 & 1 \end{pmatrix}, \quad (\text{A13})$$

where we introduce the dimensionless frequency

$$\tilde{\omega} = \frac{r_0}{a}\omega. \quad (\text{A14})$$

Eliminating \mathbf{w} between equations (A7) and (A8), we arrive at a system of differential equations for \mathbf{v} alone:

$$\frac{d\mathbf{v}}{d\tilde{r}} = (\mathbf{A}_{vv} - \mathbf{A}_{vw}\mathbf{A}_{ww}^{-1}\mathbf{A}_{wv})\mathbf{v} \equiv \mathbf{Av}, \quad (\text{A15})$$

where the second equality serves to define the overall Jacobian matrix \mathbf{A} . Although we do not write out an explicit expression for the elements of \mathbf{A} , we note that each contains a factor

$$F = \frac{1}{\beta\tilde{r}^2\tilde{\omega}^2 - 2m^2} = \frac{1}{\beta\tilde{r}^2(\tilde{\omega}^2 - \tilde{\omega}_A^2)}, \quad (\text{A16})$$

where

$$\tilde{\omega}_A = \frac{r_0}{a}\omega_A \quad (\text{A17})$$

is the dimensionless equivalent of the Alfvén frequency defined in equation (61). The factor F diverges if $\tilde{\omega} = \tilde{\omega}_A$, indicating a local resonance with the Alfvén wave. In the present context, such behavior is not a problem because we are interested in finding unstable modes for which $\tilde{\omega}^2 < 0$, and therefore the resonance never arises.

Together with the boundary conditions

$$v_1 = \tilde{\xi}_r = 0 \quad (\text{A18})$$

on the inner ($\tilde{r} = \tilde{r}_a$) and outer ($\tilde{r} = \tilde{r}_b$) boundaries of the calculation domain (in accordance with equation 41), the system of equations (A15) is a linear two-point boundary eigenvalue problem (BVEP), with $\tilde{\omega}^2$ serving as the eigenvalue. To solve the BVEP numerically we use the GYRE code (Townsend & Teitler 2013). Although GYRE is designed to address stellar pulsation problems, it is built on a robust multiple-shooting scheme which can in principle be applied to any BVEP. Accordingly, we modify GYRE to implement the differential equations and boundary conditions given here. The modified code takes as inputs parameters specifying the equilibrium model (β, γ, q), the wavenumbers (m, k), and the calculation domain (\tilde{r}_a, \tilde{r}_b , and the number of points N used to discretize the differential equations). As outputs, it calculates the eigenvalues $\tilde{\omega}^2$ of the discrete modal solutions, and the corresponding eigenfunctions given by the components of \mathbf{v} and \mathbf{w} .